

## Calculation of High Field Electron Transport Properties in InN in Comparison with GaN

H. Arabshahi, Z. Moodi and M. R. Benam

Faculty of Sciences, Payame Noor University, P. O. Box 19395-3697, Tehran, Iran

**Abstract—** Electron transport properties in InN and GaN are calculated for different temperature, doping dependencies at high electric field applications. The calculations are performed using a three valleys ensemble Monte Carlo model that includes numerical formulations of the phonon scattering rates and ionized impurity scattering rates. For two materials, we find that electron velocity overshoot only occurs when the electric field is increased to a value above a certain critical field. This critical field is strongly dependent on the material parameters. Results from the two materials are finally compared. The agreement with the available experimental data is found to be satisfactory.

**Keywords-:** Monte Carlo method; ionized impurity scattering; overshoot velocity.

### I. INTRODUCTION

InN and GaN semiconductors are becoming of increasing importance in many emerging optoelectronic and electronic device applications. Among these applications are ultraviolet photodetectors, blue and UV light emitters, and high frequency, high power electronic devices. As an aid to the device-related work, the transport coefficients of the materials need careful investigation. Transport properties of electrons in InN and GaN semiconductors can be conveniently derived by direct solution of the Boltzmann equation [1]. Previous applications of this technique were directed toward calculations of drift mobility in ideally pure semiconductors. There is also considerable interest in accurate descriptions of impure crystals, from both the experimental and the theoretical points of view. In the former case, for example, one may take advantage of the sensitivity of mobility to ionized impurities in analyses of impurity content. In the latter case, highly doped materials allow one to probe regions of the conduction band in the neighborhood of the Fermi level, well above the band edge. Obviously, accurate calculations in conjunction with experimental data are helpful in exposing weaknesses of the theoretical model, particularly with regard to electron scattering by ionized impurities at low temperatures [2]. The purpose of the present paper is to calculate electron drift velocity for various temperatures and ionized-impurity concentrations. The formulation itself applies only to the central  $\Gamma$  valley conduction band and the two nearest valleys. We have also consider band nonparabolicity, admixture of p-

type valence-band wave functions, degeneracy of the electron distribution to any arbitrary degree, and the screening effects of free carriers on the scattering probabilities [3]. All the relevant scattering mechanisms, including the two-mode nature of the polar optic phonon scattering, are taken into account [4].

In this communication, we present Monte Carlo calculations of steady-state electron transport conditions in InN and GaN [5]. We demonstrate the effect of injection energy and electric field on the electron transport properties.

This paper is organized as follows. Details of the employed simulation model is presented in section 2 and the results of steady-state electron transport properties carried out on InN and GaN structures are interpreted in section 3.

### II. MODEL DETAILS

In order to calculate the electron drift velocity for large electric fields, consideration of conduction band satellite valleys is necessary. The first-principles band structure of wurtzite InN and GaN predicts a direct band gap located at the  $\Gamma$  point and lowest energy conduction band satellite valleys at the U point and at the K point. In our Monte Carlo simulation, the  $\Gamma$  valley, the two equivalent U valleys, the six equivalent K valleys, are represented by ellipsoidal, nonparabolic dispersion relationships of the following form [6],

$$E(k)[1 + \alpha_i E(k)] = \frac{\hbar^2 k^2}{2m^*} \quad (1)$$

where  $m^*$  is effective mass at the band edge and  $\alpha_i$  is the non-parabolicity coefficient of the  $i$ -th valley. The band structure and material parameters necessary for calculating the scattering probabilities used in the present Monte Carlo simulation are used from references 1 to 4. Scattering mechanisms included in the simulation are acoustic deformation potential scattering (treated either as an elastic process or as an inelastic process) and piezoelectric scattering. Furthermore, longitudinal optical phonon scattering, nonequivalent and, where applicable, equivalent intervalley scattering events are taken into account among all valley types with the transfers assumed to be governed by the same deformation potential fields and the same phonon frequencies. Degeneracy effects are expected to be negligible over almost all of the temperature and electron concentration ranges of interest here and, hence, are not considered in the calculation. In our model at the start of each simulation, ten thousand electron particles are distributed in

momentum space according to a Maxwell-Boltzmann distribution function. These particles are propagated classically between collisions according to their velocity, effective mass and the prevailing field. The selection of the propagation time, scattering mechanism and other related quantities is achieved by generating random numbers and using this numbers to select, for example, a scattering mechanism. In the case of the ellipsoidal, non-parabolic conduction valley model, the usual Herring-Vogt transformation matrices are used to map carrier momenta into spherical valleys when particles are drifted or scattered. Steady-state results of high field transport studies have been obtained for lattice temperatures up to 600 K, in order to gain some insight into the hot carrier transport and the energy distribution function that would be generated in the gate-drain region of a power field effect transistor.

### III. RESULTS

Electron drift velocity as a function of electric field is important in determining the performance of high-speed and microwave semiconductor devices. Here we show the results of temperature dependence of the steady-state velocity-field characteristics and valley occupancy in bulk InN and GaN materials.

Figure 1 shows the simulated velocity-field characteristics at 300 K, with a background doping concentration of  $10^{17} \text{ cm}^{-3}$ , and with the electric field applied along the c-axes.

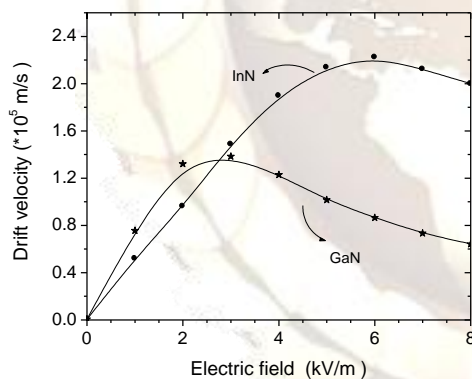


Fig 1. Calculated steady-state electron drift velocity in bulk wurtzite InN and GaN using non-parabolic band models.

Similar to the experimental results the simulations suggest that the peak drift velocity for zincblende GaAs is  $\sim 2.2 \times 10^5 \text{ ms}^{-1}$  while that for InN is about  $1.24 \times 10^5 \text{ ms}^{-1}$ . At higher electric fields, intervalley optical phonon emission dominates, causing the drift velocity to saturate at around  $0.73 \times 10^5 \text{ ms}^{-1}$  for InN and  $1.65 \times 10^5 \text{ ms}^{-1}$  for GaN. The calculated high field electron drift velocity apparent from figure 1 is fractionally lower than those that have been simulated by experimental works which assumed an effective mass in the upper valleys equal to the free electron mass. The threshold field for the onset of significant scattering into satellite conduction band valleys is a function of

the intervalley separation and the density of electronic states in the satellite valleys. The importance of electron intervalley transfer at high electric fields can be clearly seen in figure 2. In this figure the fractional valley occupancies for different materials is plotted. It is obvious that the inclusion of satellite valleys in the simulations is important. Significant electron transfer to the upper valleys only begins to occur when the field strength is very close to the threshold value. At the threshold field the electron valley occupancies at room temperature for  $\Gamma$ , U and K are about %84, %14 and %2, respectively.

Figure 3 shows the calculated electron drift velocity as a function of electric field strength for temperatures of 300, 450 and 600 K.

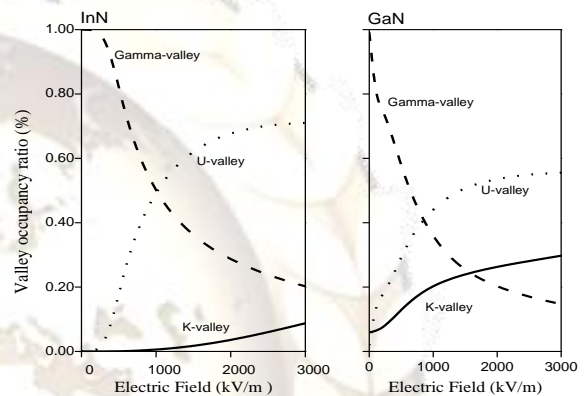


Fig 2. Fractional occupation of the central and satellite valleys in InN and GaN as a function of applied electric field using the non-parabolic band model.

The decrease in drift mobility with temperature at low fields is due to increased intravalley polar optical phonon scattering whereas the decrease in velocity at higher fields is due to increased intra and intervalley scattering. It can be seen from the figure that the peak velocity also decreases and moves to higher electric field as the temperature is increased. This is due to the general increase of total scattering rate with temperature, which suppresses the electron energy and reduces the population of the satellite valleys. This latter effect is apparent from the fact that the electron population in the central  $\Gamma$ -valley increases with temperature as shown in figure 2.

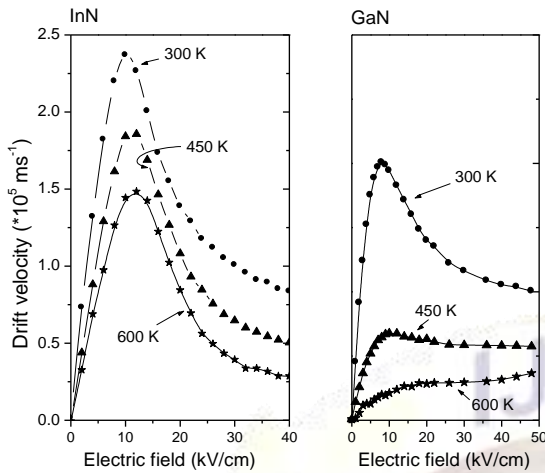


Fig 3. Calculated electron steady-state drift velocity in bulk InN and GaN as a function of applied electric field at various lattice temperatures and assuming a donor concentration of  $10^{17} \text{ cm}^{-3}$ . The peak drift velocity decreases while the threshold field increases by same percent as the lattice temperature increases from 300 to 600 K.

Figure 4 shows how the electron occupancy ratios changes with temperature for electrons in the most populated  $\Gamma$  and U valleys. There are significant statistical fluctuations in the results for the electrons in the K valleys for fields around  $500 \text{ kV m}^{-1}$ , which are caused by the relatively small number of electron particles occupying the valleys just above the threshold for intervalley transfer. Nevertheless it can be seen that the number of electrons decreases as the temperature increases for both valleys. Comparison of the temperature dependence of the valleys occupancy in InN and GaN materials show that the change in peak velocity of InN from 300 K to 600 K is a reduction of about %45 whereas for GaN it is about %25. The reason can be explained in terms of the energy band structure. In particular, the different electron effective mass within the central valley. This is important because electrons which are near a valley minimum have small kinetic energies and are therefore strongly scattered. It is apparent that intervalley transfer is substantially larger in InAs over the range of applied electric fields shown, due to the combined effect of a lower  $\Gamma$  effective mass, lower satellite valley separation energy, and slightly lower phonon scattering rate within the  $\Gamma$  valley.

Therefore, the electron velocity in InN is less sensitive to temperature than in GaN, so InN devices are expected to be more tolerant to self-heating and high ambient temperature.

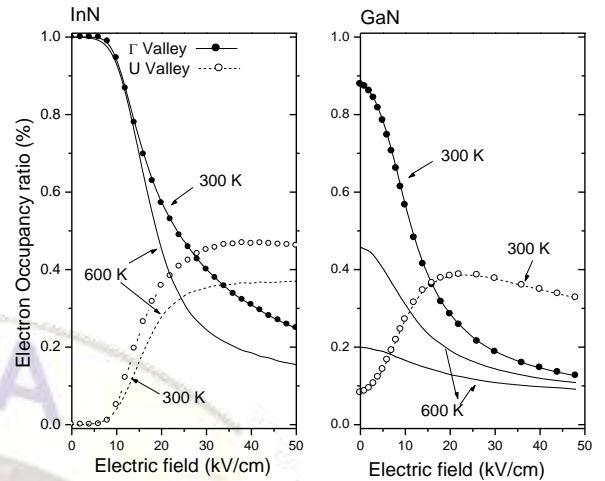


Fig 4. Temperature dependence of the valley occupancy in the  $\Gamma$  and U valleys of InN and GaN materials as a function of applied electric field.

Figure 5 shows how the velocity-field characteristic of InN and GaN materials change with impurity concentration at 300 K. It is clear that with increasing donor concentration, there are reduction in the average peak drift velocity and the threshold field because of increasing scattering rate events. The results show the trend expected from increased ionized impurity scattering is in good general agreement with recent calculations by other workers.

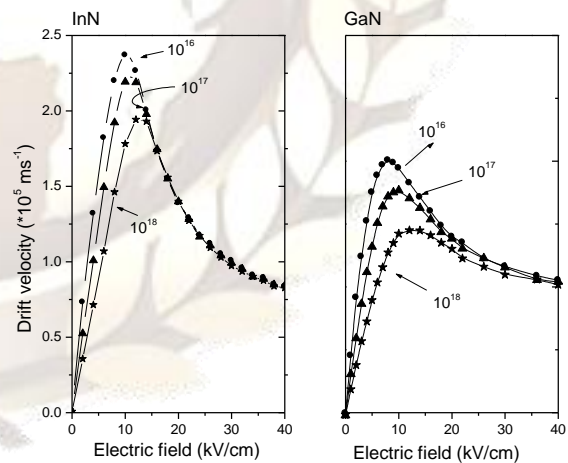


Fig 5. Calculated electron steady-state drift velocity in bulk InN and GaN as a function of applied electric field at various donor concentration up to  $10^{18} \text{ cm}^{-3}$  at room temperature.

## REFERENCES

- [1] G. W. Turner, S. J. Eglash and A. J. Strauss, " Comparison of High Field Steady State and Transient Electron Transport in Wurtzite GaN, AlN and InN", J. Vac. Sci. Technol. B, 11, (1993), pp. 864-870.

- [2] J. E. Maslar, W. S. Hurst and C. A. Wang, "The Effect of Strain Rate Variations on the Microstructure and Hot Deformation Behaviour of AA2024 Aluminium Alloy", *Appl. Spectrosc.*, 61, (2007), pp.1093-1098.
- [3] H. S. Bennett, H. Hung and A. Heckert, "Calculation of Electron Hall Mobility in GaSb, GaAs and GaN Using an Iterative Method", *J. Appl. Phys.*, 98, (2005), pp. 103705-103709.
- [4] J. R. Meyer, C. A. Hoffman, F. J. Bartoli and L. R. Ram-Mohan," Comparison of Steady-State and Transient Electron Transport in InAs, InP and GaAs", *Appl. Lett.*, 67, (1995), pp. 2756-2762.
- [14] H. Xie, W. I. Wang, J. R. Meyer and L. R. Ram-Mohan, "Comparison of High and Low Field Electron Transport in AlGaIn, AlN and GaN", *Appl. Phys. Lett.*, 65, (1994), pp.2048-2052.
- [5] H. Arimoto, N. Miura, J. R. Nichola, N. J. Mason and P. J. Walker, "Comparison of Low Field Electron Transport in SiC and GaN Structures for High-Power and high Temperature Device Modeling", *Phys. Rev. B.*, 58, (1998), pp. 4560-4566.
- [6] N. Bouarissa, A. Zaoui, J. P. Dufour, M. Certier and H. Aourag, "Discretization Method of Hydrodynamic for simulation of GaN MESFETs", *Mater. Sci. Eng. B*, 47, (1997), pp.1-7.
- [7] T. Wang, F. Kieselung and A. Forchel, "Potential Performance of SiC and GaN Based Metal Semiconductor Field Effect Transistors", *Phys. Rev. B*, 58, (1998), pp.3594-3599.
- [8] H. Arabshahi, "Comparison of SiC and ZnO Field Effect Transistors for High Power Applications", *Modern Physics Letters B*, 20, (2006), pp.787-793.
- [9] H. Arabshahi, "The Frequency Response and Effect of Trap Parameters on The Charactersitics of GaN MESFETs", *The Journal of Damghan University of Basic Sciences*,1, (2007), pp.45-49.